

A photoelectron imaging study of the deprotonated GFP chromophore anion and RNA fluorescent tags[†]

Joanne L. Woodhouse^a, Alice Henley^a, Ross Lewin^a, John M. Ward^b, Helen C.
Hailes^a, Anastasia V. Bochenkova^c, and Helen H. Fielding^{a*}

^a*Department of Chemistry, University College London, United Kingdom*

^b*Department of Biochemical Engineering, UCL, Bernard Katz Building, Gordon Street,
London WC1E 0AH, U.K*

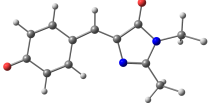
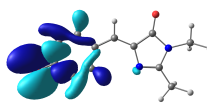
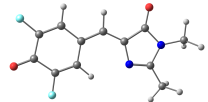
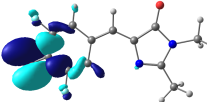
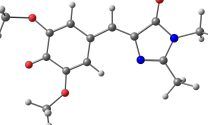
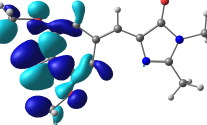
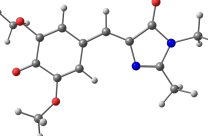
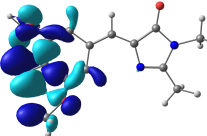
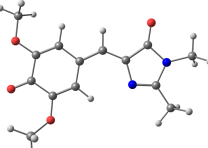
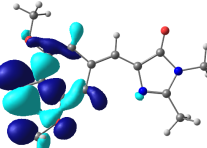
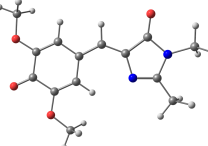
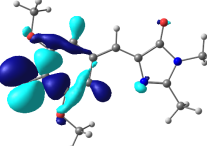
^c*Department of Chemistry, Lomonosov Moscow State University, 119991 Moscow, Russia*

E-mail: h.h.fielding@ucl.ac.uk

Supplementary Information

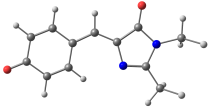
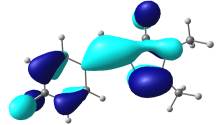
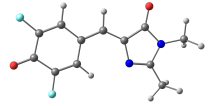
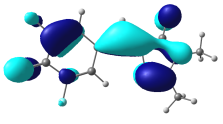
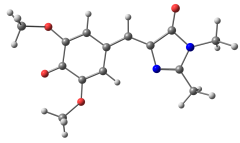
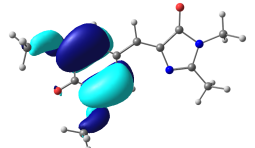
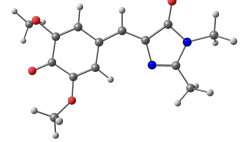
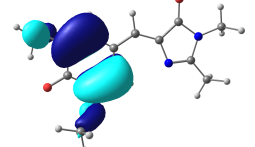
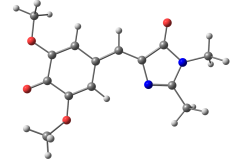
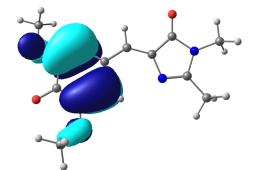
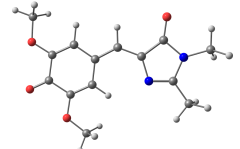
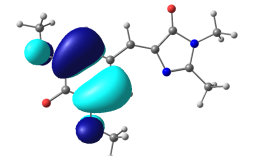
EOM-IP-CCSD D_{1n} VDEs and Orbital Holes

Table S1: B3LYP/6-311G++(3df,3pd) optimised structures, EOM-IP-CCSD VDEs and corresponding D_{1n} hole orbitals for p -HBDI⁻, DF-HBDI⁻ and all possible rotamers of DM-HBDI⁻. For p -HBDI⁻ and DF-HBDI⁻, the EOM-IP-CCSD calculations were carried out using the aug-cc-pVDZ basis set whereas a smaller 6-311G++(d,p) basis set was used for DM-HBDI⁻. The D_{1n} hole orbitals correspond to the Fock orbitals which contribute most strongly to the S_0-D_{1n} detachment transition.

Anion	Structure	$E_{\text{rel}}/$ eV	D_{1n} VDE/ eV	D_{1n} Hole
p -HBDI ⁻		-	4.50	
DF-HBDI ⁻		-	5.06	
<i>syn</i> -DM-HBDI ⁻		0	4.48	
<i>anti</i> -DM-HBDI ⁻		0	4.52	
DM-HBDI ⁻ (1 H-bond)		0.06	4.54	
DM-HBDI ⁻ (No H-bonds)		0.09	4.64	

EOM-IP-CCSD D_1 VDEs and Orbital Holes

Table S2: B3LYP/6-311G++(3df,3pd) optimised structures, EOM-IP-CCSD VDEs and corresponding D_1 hole orbitals for p -HBDI⁻, DF-HBDI⁻ and all possible rotamers of DM-HBDI⁻. For p -HBDI⁻ and DF-HBDI⁻, the EOM-IP-CCSD calculations were carried out using the aug-cc-pVDZ basis set whereas a smaller 6-311G++(d,p) basis set was used for DM-HBDI⁻. The D_1 hole orbitals correspond to the Fock orbitals which contribute most strongly to the S_0 - D_1 detachment transition.

Anion	Structure	$E_{\text{rel}}/$ eV	D_1 VDE/ eV	D_1 Hole
p -HBDI ⁻		-	4.90	
DF-HBDI ⁻		-	5.18	
<i>syn</i> -DM-HBDI ⁻		0	4.79	
<i>anti</i> -DM-HBDI ⁻		0	4.78	
DM-HBDI ⁻ (1 H-bond)		0.06	4.70	
DM-HBDI ⁻ (No H-bonds)		0.09	4.63	

Indirect detachment signal: $p\text{-HBDI}^-$ in Ar

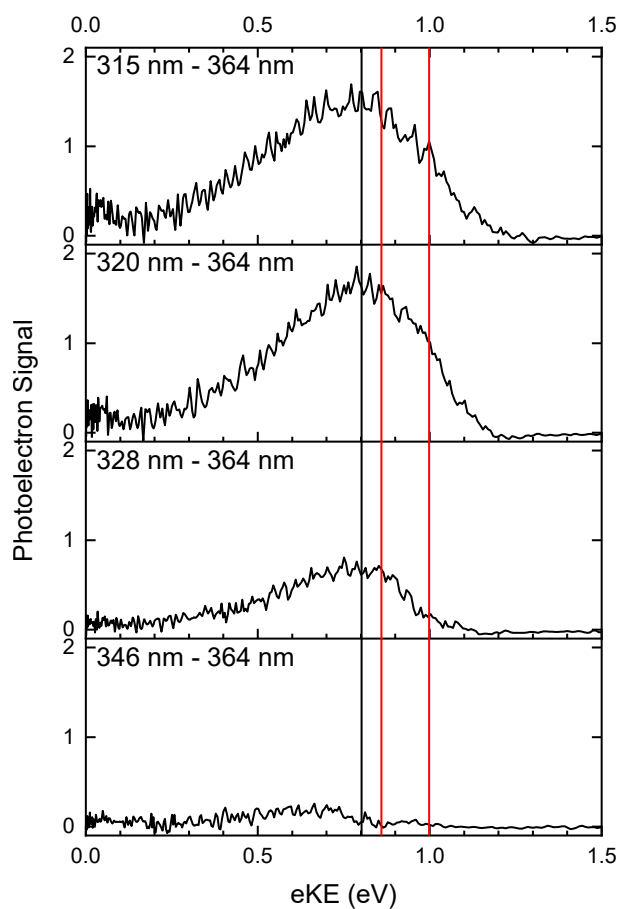


Figure S1: Difference photoelectron spectra of $p\text{-HBDI}^-$ created by subtracting the 364 nm spectral profile from the photoelectron spectra at the specified wavelengths. As such, these spectra highlight indirect detachment processes. The red lines mark the assigned eKEs corresponding to approximate AEEs of the resonant features referred to in the paper. The black line marks the maximum in the signal. Data recorded using Ar collision gas.

Indirect detachment signal: $p\text{-HBDI}^-$ in He

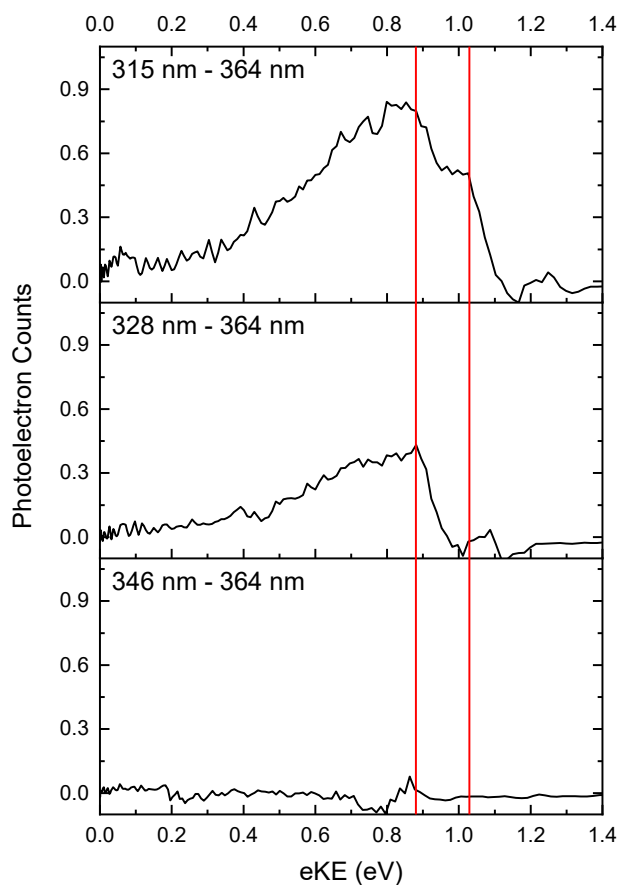


Figure S2: Difference photoelectron spectra of $p\text{-HBDI}^-$ created by subtracting the 364 nm spectral profile from the photoelectron spectra at the specified wavelengths. As such, these spectra highlight indirect detachment processes. The red lines mark the assigned eKEs corresponding to approximate AEEs of the resonant features referred to in the paper. Data recorded using He collision gas.

Indirect detachment signal: DF-HBDI⁻ in Ar

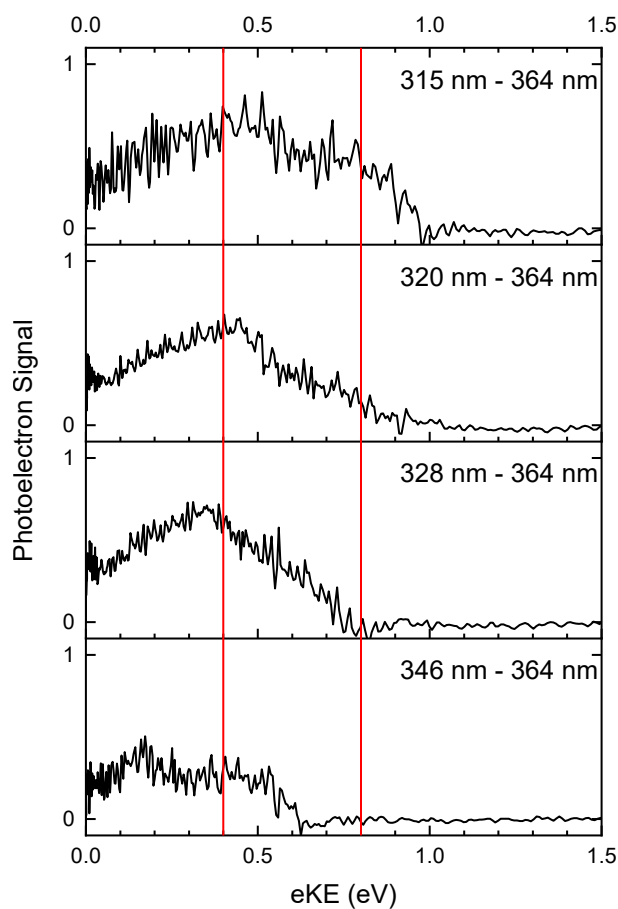


Figure S3: Difference photoelectron spectra of DF-HBDI⁻ created by subtracting the 364 nm spectral profile from the photoelectron spectra at the specified wavelengths. As such, these spectra highlight indirect detachment processes. The red lines mark the assigned eKEs corresponding to approximate AEEs of the resonant features referred to in the paper. Data recorded using Ar collision gas.

Indirect detachment signal: DM-HBDI⁻ in Ar

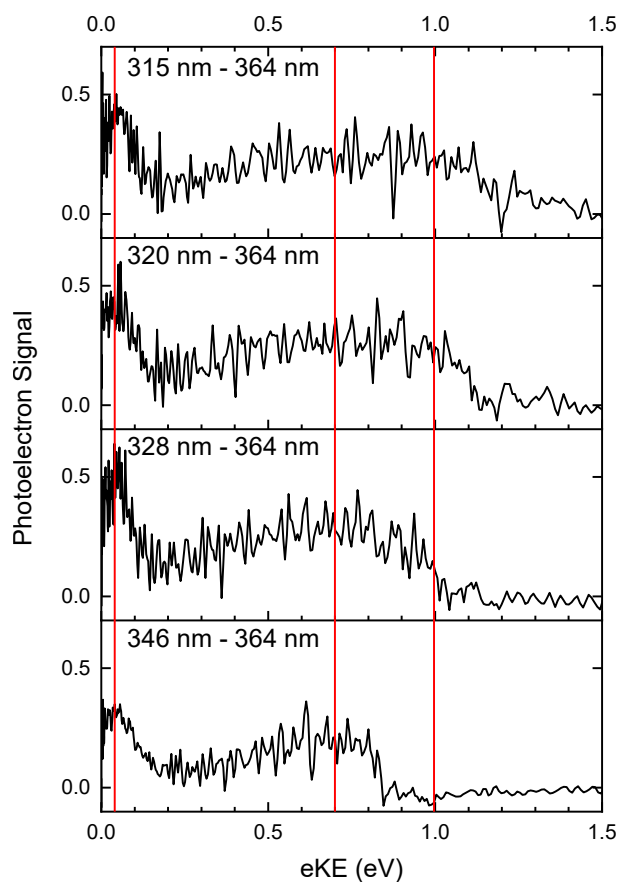


Figure S4: Difference photoelectron spectra of DM-HBDI⁻ created by subtracting the 364 nm spectral profile from the photoelectron spectra at the specified wavelengths. As such, these spectra highlight indirect detachment processes. The red lines mark the assigned eKEs corresponding to approximate AEEs of the resonant features referred to in the paper. Data recorded using Ar collision gas.

Benchmarking of 6-311G++(d,p) basis set for EOM-IP-CCSD and ezDyson Calculations

EOM-IP-CCSD/6-311G++(d,p) and EOM-IP-CCSD/aug-cc-pVDZ calculations were run using the B3LYP/6-311G++(3df,3pd) optimised structure of PhO^- which yielded consistent vertical detachment energies to D_0 of 1.99 eV and 2.06 eV, respectively. The resulting Dyson orbitals were used as inputs to the ezDyson program, the resulting β_2 parameters as a function of eKE are presented in Fig. S5. It can be seen that, while the results are not exactly the same, the magnitude and the expected trend in β_2 as a function of eKE is consistent between the two basis sets, with the largest discrepancy between individual β_2 values being ~ 0.05 .

EOM-IP-CCSD/6-311G++(d,p) and EOM-IP-CCSD/aug-cc-pVDZ calculations were run using the B3LYP/6-311G++(3df,3pd) optimised structure of $p\text{-HBDI}^-$ which yielded consistent vertical detachment energies to D_0 of 2.61 eV and 2.66 eV, respectively. The resulting Dyson orbitals were used as inputs to the ezDyson program, the resulting β_2 parameters as a function of eKE are presented in Fig. S5. It can be seen that the magnitude and expected trend in β_2 as a function of eKE is similarly consistent between the two basis sets, with the largest discrepancy between individual β_2 values being ~ 0.05 .

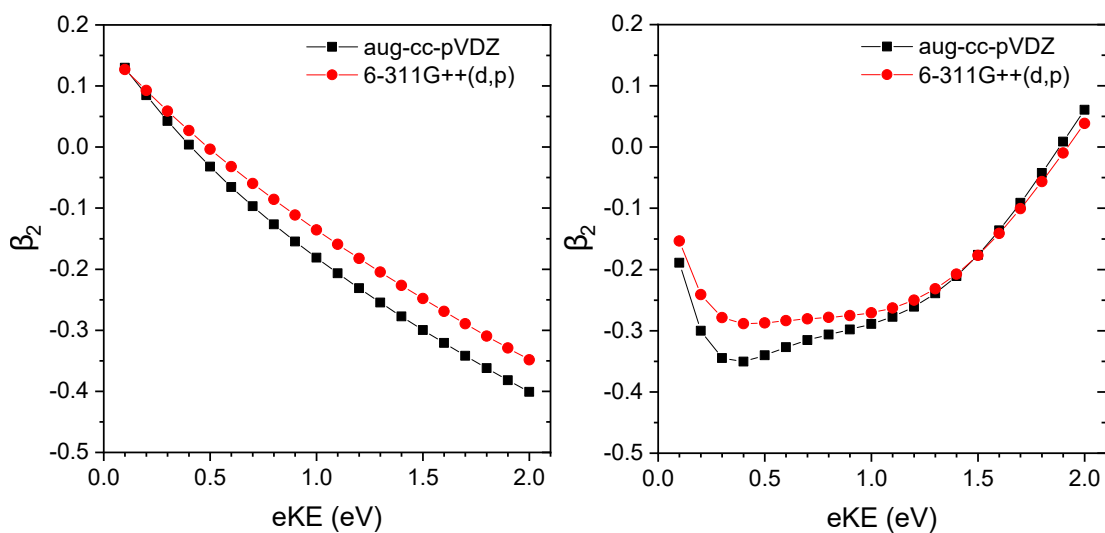


Figure S5: ezDyson calculated β_2 parameters as a function of electron eKE for PhO^- (left) and $p\text{-HBDI}^-$ (right). The ezDyson calculation used Dyson orbitals from EOM-IP-CCSD calculations with the specified basis sets and $l_{\text{max}} = 5$.

Beta Parameters for DF-HBDI⁻ at 346 nm - 364 nm

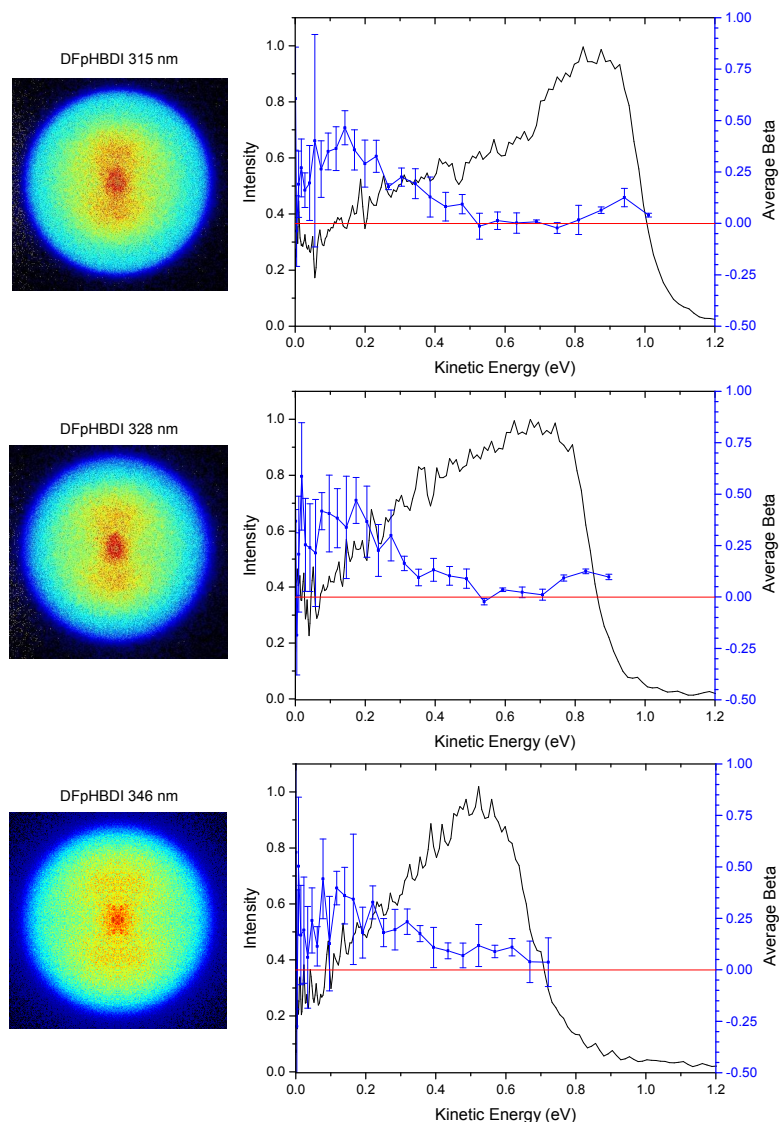


Figure S6: Photoelectron images and photoelectron spectra of the DF p -HBDI⁻ anion produced by electrospray ionisation at the specified wavelengths plotted as a function of eKE (black line). The β_2 values were averaged over every five data points and are plotted to coincide with the corresponding eKEs (blue squares); the error bars give the standard deviation. $\beta_2 = 0$ has been marked with a horizontal red line for comparison. The photoelectron images have been oriented such that the vertical axis is parallel with the polarisation vector of the laser light.

Beta Parameters for DM-HBDI⁻ at 346 nm - 364 nm

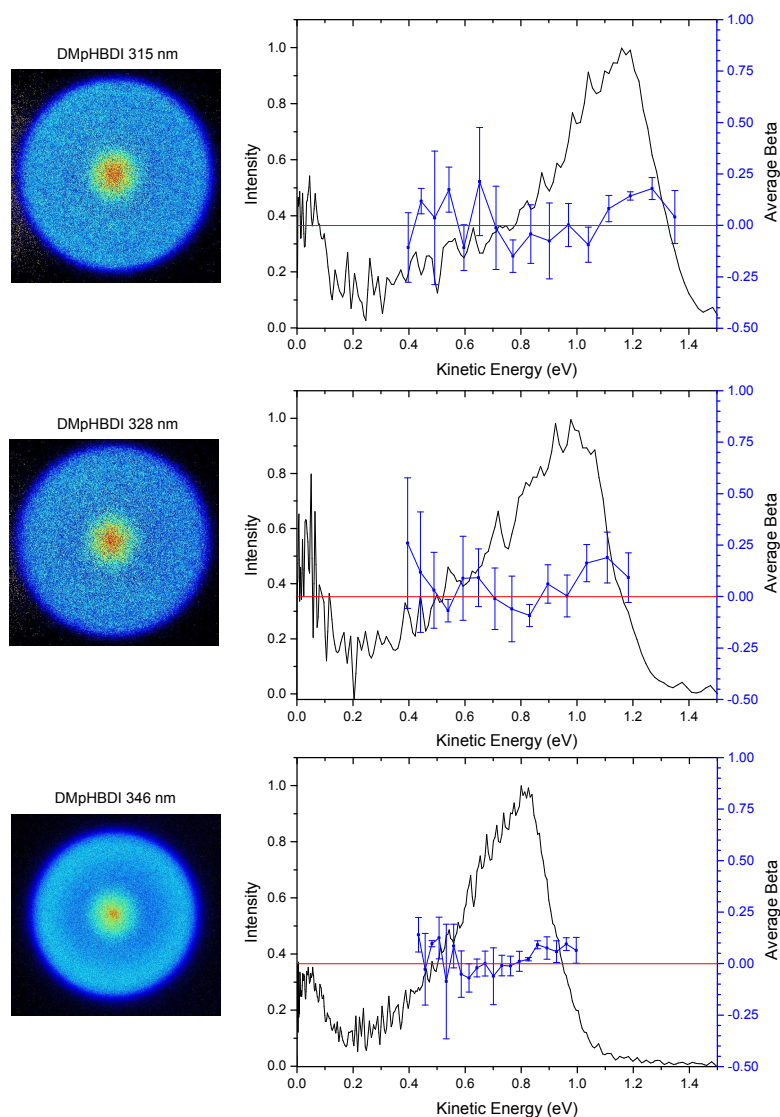


Figure S7: Photoelectron images and photoelectron spectra of the DM p -HBDI⁻ anion produced by electrospray ionisation at the specified wavelengths plotted as a function of eKE (black line). The β_2 values were averaged over every five data points and are plotted to coincide with the corresponding eKEs (blue squares); the error bars give the standard deviation. $\beta_2 = 0$ has been marked with a horizontal red line for comparison. The photoelectron images have been oriented such that the vertical axis is parallel with the polarisation vector of the laser light.

ezDyson calculation for all DM-HBDI⁻ rotamers

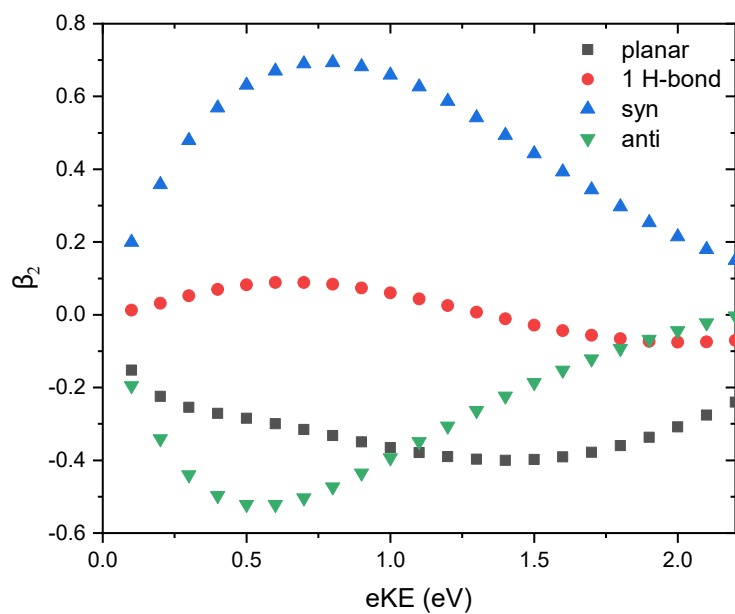


Figure S8: ezDyson calculated β_2 parameters for S_0 - D_0 direct detachment process for the four rotamers of DM-HBDI⁻ as a function of eKE. EOM-IP-CCSD/6-311G++(d,p) orbitals were used as input.